Supporting Information for:

Enhancement of Macromolecular Ice Recrystallisation Inhibition Activity by Exploiting Depletion Forces

Toru Ishibe[a], Thomas Congdon[a], Christopher Stubbs[a], Muhammad Hasan[b], Gabriele C. Sosso[a,c] and Matthew I. Gibson[a,b]*

[a]Department of Chemistry, University of Warwick Coventry, UK, CV4 7AL, [b]Warwick Medical School, University of Warwick, Coventry, UK, CV4 7AL, [c]Centre for Scientific Computing, University of Warwick, Coventry, UK, CV4 7AL.

* E-mail: M.I.Gibson@warwick.ac.uk (M. I. Gibson).

Experimental Section

Materials

Poly(ethylene glycol) (PEG) (4kDa), acrylic acid (AA), methacrylic acid (MA), safranin-O, 2-cyano-2-propyl dodecyltrithiocarbonate and NaCl were purchased from Sigma-Aldrich and used as supplied unless otherwise stated. Phosphate-buffered saline (PBS) solutions were prepared using pre-formulated tablets (Sigma-Aldrich) in 200 mL of Milli-Q water (>18.2 Ω mean resistivity) to give [NaCl] = 0.138 M, [KCl] = 0.0027 M, and pH 7.4. Poly(vinyl alcohol) (PVA_{85}) (3.7kDa)[1] and Poly(vinylpyrrolidone)[2] were synthesised as previously reported. AFGP8 was provided by A. L. DeVries, University of Illinois at Urbana-Champaign, USA. 2,5-dioxopyrrolidin-1-yl 2-((ethoxycarbonothioyl)thio)-2-methylpropanoate (MADIX-NHS) was also synthesised as reported previously.[1]

Physical and Analytical Methods

Samples for western blot analysis were resolved on a polyacrylamide gel, transferred to a membrane and detected a using primary (monoclonal anti-polyhistidine) antibody and a secondary (goat anti-mouse IgG (H+L)) antibody. Fast protein liquid chromatography (FPLC) was performed using AKTA pure (GE Healthcare) with a flow rate of 1 $mL.min^{-1}$ using PBS buffer.

Ice wafers were annealed on a Linkam Biological Cryostage BCS196 with T95-Linkpad system controller equipped with a LNP95-Liquid nitrogen cooling pump, using liquid nitrogen as the coolant (Linkam Scientific Instruments UK, Surrey, UK). An Olympus CX41 microscope equipped with a UIS-2 20x/0.45/∞/0-2/FN22 lens (Olympus Ltd, Southend on sea, UK) and a Canon EOS 500D SLR digital camera was used to obtain all images. Image

processing was conducted using ImageJ, which is freely available from http://imagej.nih.gov/ij/.

^{1}H and ^{13}C NMR spectra were recorded on Bruker Avance III HD 300 MHz or HD 400 MHz spectrometers using deuterated solvents obtained from Sigma-Aldrich. Chemical shifts are reported relative to residual non-deuterated solvent.

The size exclusion chromatography (SEC) in DMF is comprised of an Agilent 390-LC MDS instrument equipped with differential refractive index (DRI), viscometry (VS), dual angle light scatter (LS) and UV detectors. The system was equipped with 2 x PLgel Mixed D columns (300 x 7.5 mm) and a PLgel 5 µm guard column. The eluent is DMF with 5 mmol NH_4BF_4 additive. Samples were run at 1 ml/min at 50 °C. Poly(methyl methacrylate) standards (Agilent EasyVials) were used for calibration between 955,000 – 550 g/mol. Analyte samples were filtered through a nylon membrane with 0.22 µm pore size before injection. Respectively, experimental molar mass (Mn, SEC) and dispersity (Đ) values of synthesized polymers were determined by conventional calibration and universal calibration using Agilent GPC/SEC software.

The size exclusion chromatography (SEC) in THF is comprised of an Agilent 390-LC MDS instrument equipped with differential refractive index (DRI), viscometry (VS), dual angle light scatter (LS) and dual wavelength UV detectors. The system was equipped with 2 x PLgel Mixed C columns (300 x 7.5 mm) and a PLgel 5 µm guard column. The eluent is THF with 2 % TEA (triethylamine) and 0.01 % BHT (butylated hydroxytoluene) additives. Samples were run at 1 mL/min at 30 °C. Poly(methyl methacrylate) and polystyrene standards (Agilent EasyVials) were used for calibration. Analyte samples were filtered through a GVHP membrane with 0.22 µm pore size before injection. Respectively, experimental molar mass (Mn, SEC) and dispersity (Đ) values of synthesized polymers were determined by conventional calibration using Agilent GPC/SEC software.

The size exclusion chromatography (SEC) in aqueous is comprised of an Agilent Technologies Infinity 1260 MDS instrument equipped with a differential refractive index (DRI), light scattering (LS) and viscometry (VS) and UV detectors. The column set used were Tosoh TSKGel GPWXL *2. The mobile phase used was 0.1 M $NaNO_3$. Columnoven and detector temperatures were regulated to 40 °C, flow rate 1 mL/min (These change regularly – please check). Poly(ethyleneoxide) standards (Agilent EasyVials) were used for calibration between 1,368,000 – 106 g/mol. Analyte samples were filtered through a hydrophilic GVWP membrane with 0.22 μm pore size before injection. Respectively, experimental molar mass (Mn, SEC) and dispersity (Đ) values of synthesized polymers were determined by conventional calibration using Agilent GPC/SEC software.

Ice Recrystallisation Inhibition (Splat) Assay

A 10 μL sample of polymer dissolved in PBS buffer (pH 7.4) is dropped 1.40 m onto a glass microscope coverslip, which is on top of an aluminium plate cooled to −78 °C using dry ice. The droplet freezes instantly upon impact with the plate, spreading out and forming a thin wafer of ice. This wafer is then placed on a liquid nitrogen cooled cryostage held at −8 °C. The wafer is then left to anneal for 30 min at −8 °C. The number of crystals in the image is counted, again using ImageJ, and the area of the field of view divided by this number of crystals to give the average crystal size per wafer, and reported as a % of area compared to PBS control.

Depletion Effect Assay

At least six droplets (0.5 μL) of polymer dissolved in water or 2M NaCl aqueous solution is formed onto a glass (7.6cm x 2.6cm). The droplets are dried under 40% humidity for 5 min. This wafer is then washed by Milli-Q water. The wafer is then blown with N_2 gas and dried

over. The trace of remaining droplets is observed by fluorescence microscope. The green intensity of the fluorescence image is counted using ImageJ.

The following samples were tested. As the control sample, we prepared Sample 4 without washing by Milli-Q water.

1. Labelled PVA 10 mg/mL + PEG(4kDa) 10 mg/mL in 2M NaCl aqueous solution
2. Labelled PVA 10 mg/mL in 2M NaCl aqueous solution
3. Labelled PVA 10 mg/mL + PEG(4kDa) 10 mg/mL in Water
4. Labelled PVA 10 mg/mL in Water

Synthetic Methods

Synthesis of Poly(methacrylic acid)

Methacrylic acid (1.21g, 0.014 mol, 100 eq) was added to a vial containing 2-cyano 2-propyl dodecyltrithiocarbonate (47 mg, 0.14 mmol, 1 eq), sealed, and degassed by bubbling under nitrogen for 15 minutes. The vial was then exposed to blue light for 24 hours at room temperature. The resulting polymer was precipitated into diethyl ether and dried under vacuum. ^{1}H NMR (D_2O): δ = 0.93-1.31 ($CH_2C(CH_3)COOH$, br), 1.60-2.24 ($CH_2C(CH_3)COOH$, br). M_n^{SEC}(Aqueous) = 14,000 Da, M_w/M_n = 2.72.

Synthesis of Poly(acrylic acid)

Acrylic acid (1g, 0.014 mol, 100 eq) was added to a vial containing 2-cyano 2-propyl dodecyltrithiocarbonate (47 mg, 0.14 mmol, 1 eq), sealed, and degassed by bubbling under

nitrogen for 15 minutes. The vial was then exposed to blue light for 24 hours at room temperature. The resulting polymer was precipitated into diethyl ether and dried under vacuum. ^{1}H NMR ($CDCl_3$): δ = 1.00-1.63 (C*H*$_2$CHCOOH, br), 1.64-1.87 (C*H*$_2$CHCOOH, br), 2.00-2.42 (C*H*$_2$CHCOOH, br), 3.63-4.49 (CH$_2$C*H*COOH, br), 11.94-12.75 (O*H*, br). M_n^{SEC}(DMF) = 26,000 Da, M_w/M_n = 1.43. FTIR: Acid-OH 3024 (broad), C=O 1699 cm^{-1}, C-O 1448 cm^{-1}.

Synthesis of Poly(Vinyl Alcohol)-NHS Ester (PVAc-NHS)

Vinyl acetate (1 g, 0.011 mol, 500 eq) was added to a vial containing MADIX-NHS (7 mg, 0.02 mmol, 1 eq) and ACVA (1.3 mg, 0.004 mmol, 0.2 eq) and degassed by bubbling under nitrogen for 15 minutes. The sample was heated with stirring to 68 °C, and left to react for 24 hours. The resulting solution was precipitated three times into diethyl ether. The resulting yellow solid was analysed by NMR and SEC to determine molecular weight, as well as ensure incorporation of the NHS end group.

^{1}H NMR ($CDCl_3$): δ = 1.72-1.97 (C*H*$_2$CHOOCH$_3$, br), 1.98-2.15 (CH$_2$CHOOC*H*$_3$, br), 4.82-5.11 (CH$_2$C*H*OOCH$_3$, br). M_n^{SEC}(DMF) = 26,000 Da, M_w/M_n = 1.43. FTIR: C=O 1729 cm^{-1}, C-O 1370 cm^{-1}.

Synthesis of Fluorescently Labelled PVA

PVAc-NHS (100 mg, 1 eq) was dissolved in THF and stirred with TEA (50 mg) for 15 minutes, after which N-[4-(Aminomethyl)benzyl]rhodamine 6G-amide bis(trifluoroacetate) (1.4 mg, 0.2 eq) was added and stirred in the dark for 48 hours. The resulting polymer was concentrated under vacuum and precipitated twice in diethyl ether followed by dissolution in methanol (3 mL) at 60 °C, after 30 minutes, hydrazine hydrate (78-82% in water) (10 mL) was added and left to react for 24 hours after which time the sample was diluted with water and dialysed (1000 MWCO) for 48 hours (7 water changes), followed by lyophilisation. Deprotection was

confirmed by IR, and fluorescence by microscopy of a dried polymer. FTIR: Alcohol 3278 cm^{-1}, C-O 1418 cm^{-1}.

Protein Expression

AFPIII expression and purification

A pET21b plasmid encoding for a hexahistidine-tagged AFPIII was transformed into competent *Escherichia coli* BL21(DE3) cells (New England Biolabs). Single colonies were selected and grown overnight in 200 mL Lysogeny Broth (LB)-medium containing 100 μg/mL ampicillin under continuous shaking (37 °C, 180 rpm). Preculture was added (10 mL in 1 L) to LB-medium supplemented with ampicillin and grown until OD600 = 0.6. Isopropyl β-D-1-thiogalactopyranoside (IPTG) was then added to the cells to a final concentration of 0.4 mM to induce protein expression overnight (16 °C, 180 rpm). The cells were harvested by centrifugation (4 °C, 5000 g, 10 minutes), the supernatant decanted and the cells resuspended in prechilled phosphate buffered saline (PBS). Pierce protease inhibitor mini-tablets were added to the suspension and it was passed through a STANSTED 'Pressure Cell' FGP12800 homogeniser to undergo lysis. The cell lysate was centrifuged (4 °C, 40,000 g, 45 minutes) and the supernatant syringe filtered (0.45 μm) and passed through a pre-equilibrated IMAC Sepharose 6 Fast Flow (GE Healthcare) column charged with Ni(II) ions. The column was washed first with 5 column volumes of PBS, then with 3 column volumes of 20 mM imidazole in PBS. 300 mM imidazole in PBS was used to elute bound AFPIII and the protein was further purified using size-exclusion chromatography (HiLoad Superdex 75 gel filtration column). Western blot and SDS-PAGE gel electrophoresis were used to confirm the presence of AFPIII, and the protein concentration determined using Thermo Scientific Pierce BCA assay kit and verified by measuring absorbance at 280 nm and using Beer-Lambert law.

Additional Data

Figure S1 shows DLS (dynamic light scattering) measurement results. PVA forms colloidal aggregates at raised salt concentration, but PEG (poly(ethylene glycol) does not.

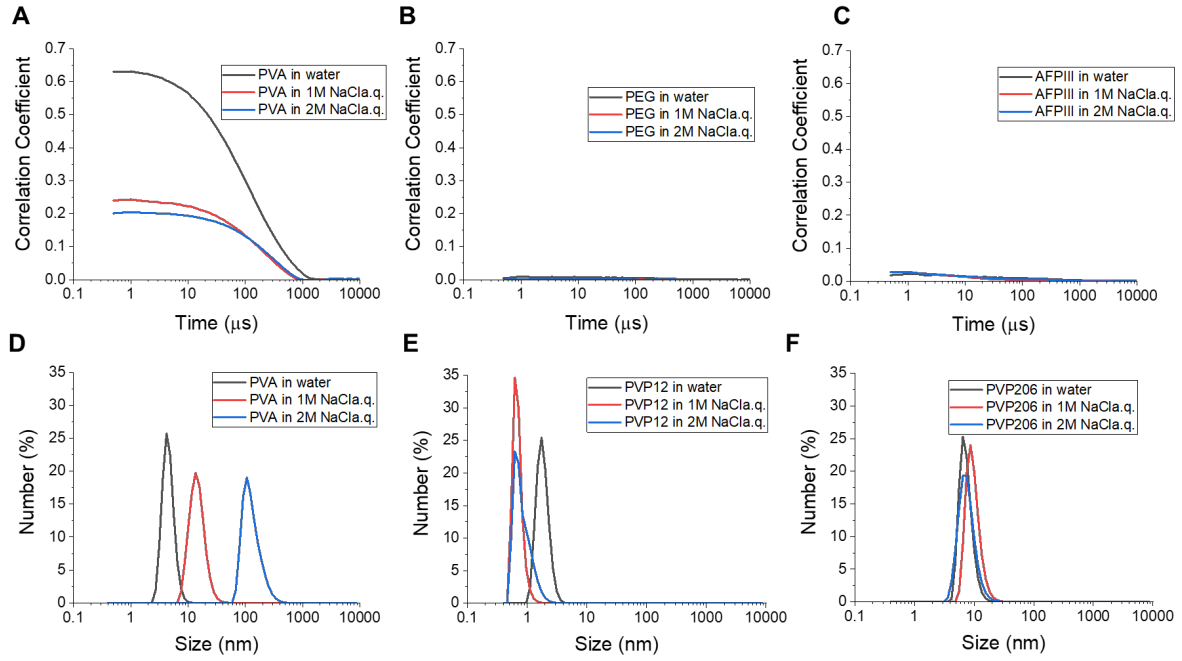

Figure S1. Measurement results of dynamic light scattering. Concentrations of all samples are 0.5 mg/mL in water, 1M NaCl aqueous solution or 2M NaCl aqueous solution. (A) Correlation Coefficient for PVA_{85}. (B) Correlation Coefficient for PEG. (C) Correlation Coefficient for AFPIII. (D) Number of particles for PVA_{85}. (E) Number of particles for PVP_{12}. (F) Number of particles for PVP_{206}.

A concentration of PVA, AFGP8, AFPIII and Safranin O giving 50% MGS is determined by Figure S2.

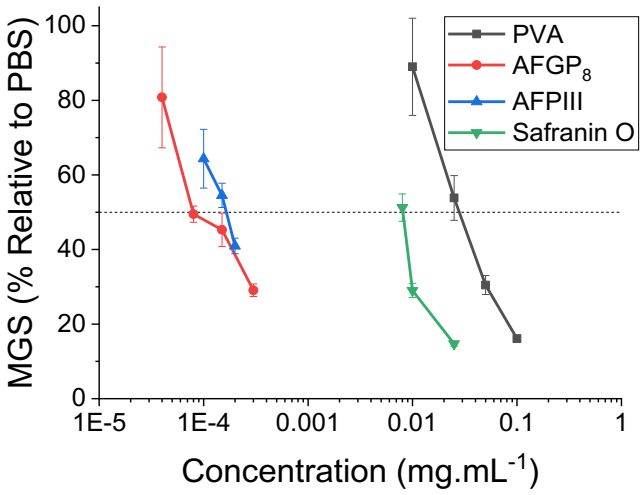

Figure S2. Comparison of mean grain size (MGS) for PVA, AFGP8, AFPIII and Safranin O.

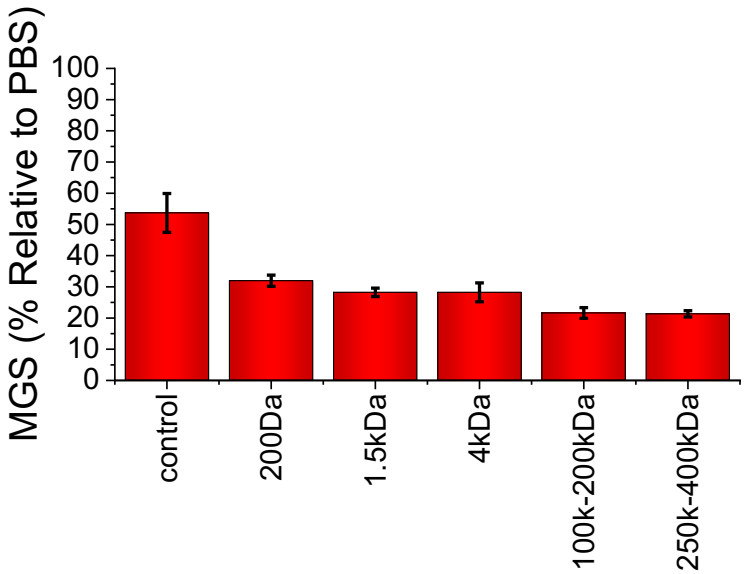

Figure S3. IRI activity for PVA with the addition of different molecular weight PEGs. 'Control' is PVA alone. [PVA_{85}] = 0.025 mg.mL^{-1}. [PEG] = 1 mg.mL^{-1}.

Theory Section

The impact of depletion forces in a PVA/PEG mixture

We consider a solution containing a certain volume concentration (or volume fraction - if assuming an ideal solution) of PVA:

$$\sigma_{\mathrm{PVA}} = \frac{V_{\mathrm{PVA}}}{V_{\mathrm{Tot.}}} \tag{1}$$

where V_{PVA} is the volume of PVA in solution and $V_{\mathrm{Tot.}}$ is the total volume of the latter. The PVA particles are treated as hard spheres colloidal particles of radius $R_{\mathrm{PVA}} = 10$ nm. In the same solution we have also a certain volume concentration of PEG (σ_{PEG}), which we treat as non interacting polymer particles of radius $R_{\mathrm{PEG}} = 1$ nm.

Assuming the solution contains a fixed amount of N particles (PVA, PEG, and solvent) in a box of fixed volume V at constant temperature T, the canonical partition function Q of the system is determined by the amount of volume $V_{acc.}^{\mathrm{PEG}}$ accessible to the PEG particles only - assuming both PEG-PEG and PVA-PEG interactions are negligible. Then,

$$V_{acc.}^{\mathrm{PEG}} = V_{\mathrm{Tot.}} - V_{\mathrm{PVA}}^{+}, \tag{2}$$

where V_{PVA}^{+} is the volume occupied by the PVA particles and their exclusion shells (i.e. the spherical shell of radius equal to R_{PEG} which are not accessible to PEG particles, as PVA and PEG particles cannot overlap). As we are interested in (Helmholtz) free energy F differences, we ignore the kinetic contribution to Q (which would end up being an additive constant to F) and proceed as follows:

$$
\begin{aligned}
F &= -k_B T \ln Q \\
&= -k_B T \ln Q_{\mathrm{PEG}} \\
&= -k_B T \ln(q_{\mathrm{PEG}}^{N_{\mathrm{PEG}}}) \\
&= -k_B T N_{\mathrm{PEG}} \ln q_{\mathrm{PEG}}
\end{aligned} \tag{3}
$$

where k_B, N_{PEG}, Q_{PEG} and q_{PEG} are the Boltzmann constant, the number of PEG particles in the solution, the canonical partition function of the system (which depends on PEG particles only), and the partition function of a single PEG particle, respectively. Note that for Eq. 3 to be valid, there must be no interaction between PEG particles at all.

If we consider just two PVA particles to be present in the solution, then we can write down q_{PEG} for two limiting cases:

- $q_{\mathrm{PEG}}(r \to \infty)$ i.e. the volume accessible to the PEG particles when the two PVA particles are separated by a distance r much larger than $R_{\mathrm{PVA}} + R_{\mathrm{PEG}}$. In this scenario, we have:

$$
q_{\mathrm{PEG}}(r \to \infty) = V_{\mathrm{Tot.}} - 2\left[\frac{4}{3}\pi(R_{\mathrm{PVA}} + R_{\mathrm{PEG}})^3\right] \tag{4}
$$

- $q_{\mathrm{PEG}}(r = 2R_{\mathrm{PVA}})$ i.e. the volume accessible to the PEG particles when the two PVA particles are in contact with each other - this is the minimum possible value of r, given that hard spheres particles cannot overlap. In this case, we have:

$$
q_{\mathrm{PEG}}(r = 2R_{\mathrm{PVA}}) = q_{\mathrm{PEG}}(r \to \infty) + \left(2\pi R_{\mathrm{PVA}} R_{\mathrm{PEG}}^2 + \frac{4}{3}\pi R_{\mathrm{PEG}}^3\right) \tag{5}
$$

, where we have taken advantage of the expression for the volume spanned by the intersection of two spheres.[3] At this point, we can ask ourselves what is the free energy difference between

the two PVA particles in contact with each other (a PVA "dimer", so to say) and the same two particles separated in solution:

$$
\begin{aligned}
F_{\text{dimer}} &= -k_B T N_{\text{PEG}} \ln q_{\text{PEG}}(r = 2R_{\text{PVA}}) + k_B T N_{\text{PEG}} q_{\text{PEG}}(r \to \infty) \\
&= -k_B T N_{\text{PEG}} \ln \left[\frac{q_{\text{PEG}}(r = 2R_{\text{PVA}})}{q_{\text{PEG}}(r \to \infty)} \right] \\
&= -k_B T N_{\text{PEG}} \ln \left[\frac{V_{\text{Tot.}} - 2\left[\frac{4}{3}\pi(R_{\text{PVA}} + R_{\text{PEG}})^3\right] + \left(2\pi R_{\text{PVA}} R_{\text{PEG}}^2 + \frac{4}{3}\pi R_{\text{PEG}}^3\right)}{V_{\text{Tot.}} - 2\left[\frac{4}{3}\pi(R_{\text{PVA}} + R_{\text{PEG}})^3\right]} \right] \\
&= -k_B T N_{\text{PEG}} \ln \left[1 + \frac{\left(2\pi R_{\text{PVA}} R_{\text{PEG}}^2 + \frac{4}{3}\pi R_{\text{PEG}}^3\right)}{V_{\text{Tot.}} - 2\left[\frac{4}{3}\pi(R_{\text{PVA}} + R_{\text{PEG}})^3\right]} \right], \text{ using } \frac{\alpha + \gamma}{\alpha} = 1 + \frac{\gamma}{\alpha} \\
&= -k_B T N_{\text{PEG}} \left[\frac{\left(2\pi R_{\text{PVA}} R_{\text{PEG}}^2 + \frac{4}{3}\pi R_{\text{PEG}}^3\right)}{V_{\text{Tot.}} - 2\left[\frac{4}{3}\pi(R_{\text{PVA}} + R_{\text{PEG}})^3\right]} \right], \text{ using } \ln(x+1) \approx x \text{ for small } x \\
&= -k_B T N_{\text{PEG}} \left[\frac{\left(2\pi R_{\text{PVA}} R_{\text{PEG}}^2 + \frac{4}{3}\pi R_{\text{PEG}}^3\right)}{V_{\text{Tot.}}} \right], \text{ assuming} V_{\text{Tot.}} >>> \frac{4}{3}\pi(R_{\text{PVA}} + R_{\text{PEG}})^3 \\
&= -k_B T \frac{N_{\text{PEG}}}{V_{\text{Tot.}}} \left[\frac{4}{3}\pi R_{\text{PEG}}^3 \left(1 + \frac{3}{2}\frac{R_{\text{PVA}}}{R_{\text{PEG}}}\right) \right] \\
&= -k_B T \sigma_{\text{PEG}} \left(1 + \frac{3}{2}\frac{R_{\text{PVA}}}{R_{\text{PEG}}}\right)
\end{aligned}
\tag{6}
$$

This expression can be found in similar forms throughout the recent literature (see e.g. Ref.[4]) and has been used in this work to study the dependence of $F_{\text{PVA dimer}}$ as a function of R_{PEG} (see Fig. 1b in the main text): is an approximation that applies to values of σ_{PEG} up to ≈30%.[5] Note that in order to obtain the volume fractions of PVA and PEG we have assumed a density of 1.19 and 1.125 g/cm^3.

PVA aggregates

Size distribution

We now focus on the formation of aggregates containing not just two, but an arbitrary number N_{ag} of PVA particles. The starting point has to be the chemical potential μ, which

- at equilibrium - has to be the same for all the PVA particles, either alone ("monomers") or within an aggregate of a given size N_{ag}. In particular, the chemical potential of PVA as a monomer, μ_1, has to be equal to the chemical potential of an aggregate containing N_{ag} PVA particles, $\mu_{N_{ag}}$. Hence:

$$\mu_1^o + \frac{k_B T}{1} \ln\left(\frac{\chi_1}{1}\right) = \mu_{N_{ag}}^o + \frac{k_B T}{N_{ag}} \ln\left(\frac{\chi_{N_{ag}}}{N_{ag}}\right) \tag{7}$$

where $\mu_{N_{ag}}^o$ is the mean interaction free energy per PVA particle in a PVA aggregate of size N_{ag} and $\chi_{N_{ag}}$ is the concentration (in fact, $\chi_{N_{ag}}$ has to be dimensionless, so it could be either a molar or volume fraction) of PVA particles which participate in aggregates containing N_{ag} PVA particles. The size distribution of the aggregates $\frac{\chi_{N_{ag}}}{N_{ag}}$ can thus be written as:

$$\frac{\chi_{N_{ag}}}{N_{ag}} = \left[\chi_1 e^{\frac{\mu_1^o - \mu_{N_{ag}}^o}{k_B T}}\right]^{N_{ag}} \tag{8}$$

Notably, the expression for $N_{ag}\mu_{N_{ag}}^o$ depends on the morphology of the aggregate - which in turn affects the extent of the excluded volume between particles and thus their interaction free energy. Here, we consider a simple scenario where PVA particles aggregate as one-dimensional chains. In this case, the excluded volume is always the same for each particle in aggregate of any size (with the exception of the two PVA particles at the start and end of the 1D chain) and identical to the excluded volume we have previously calculated for a PVA "dimer". Hence, the total interaction free energy associated with an aggregate containing N_{ag} PVA particles is:

$$\begin{aligned} F_{N_{ag},\text{chain}} &= F_{\text{dimer, in the chain}}(N_{ag}-1) = F_{\text{dimer}}(N_{ag}-1) \text{ or} \\ &= N_{ag}\mu_{N_{ag}}^o = -\alpha k_B T(N_{ag}-1), \text{ with } \alpha = -\frac{F_{\text{dimer, in the chain}}}{k_B T} = -\frac{F_{\text{dimer}}}{k_B T} \end{aligned} \tag{9}$$

Thus, the size distribution of these 1D PVA aggregates is:

$$\chi_{N_{ag}} = N_{ag}\left[\chi_1 e^{\frac{\mu_1^o - \mu_{N_{ag}}^o}{k_B T}}\right]^{N_{ag}}$$
$$= N_{ag} e^{[N_{ag}(\ln \chi_1 + \alpha)] - \alpha} \tag{10}$$

Note that nothing prevents us to reason in terms of volume fractions (as opposed to molar fractions), so that the volume fraction of PVA particles with respect to all the PVA particles in solution (not with respect to the solution as a whole!) reported in Fig. 1c (see main text) can be written as:

$$\sigma(PVA)_{\text{solution}} = N_{ag} e^{[N_{ag}(\ln \sigma_{\text{PVA}} + \alpha)] - \alpha} \tag{11}$$

Thus, in order to compute $\sigma(PVA)_{\text{solution}}$ we need to pick a given volume fraction of PVA (σ_{PVA}) as well as a given value of α, which in turn depends on σ_{PEG} and $\frac{R_{\text{PVA}}}{R_{\text{PEG}}}$.

Critical aggregation concentration

It is interesting to ask ourselves whether whether there exist a simple expression for the concentration of PVA at which further addition of PVA into the solution necessarily results in the formation of PVA aggregates, while the concentration of PVA "monomers" (i.e. single PVA particles in solution) remains basically constant. This quantity is known as the critical aggregation concentration (CAC), and plays a key role in the context of the assembly of biological entities (often under the name of critical *micelle* concentration, CMC[6,7]). A derivation of the CAC can be found in the excellent work of Israelachvili.[8] Importantly, while the CAC has to do, in principle, with the amount of PVA in solution, the final result depends on α (derived above), which in turn is a function of PEG concentration as well as $\frac{R_{\text{PVA}}}{R_{\text{PEG}}}$. We start from:

$$\frac{\chi_{N_{ag}}}{N_{ag}} = \left[\chi_1 e^{\frac{\mu_1^o - \mu_{N_{ag}}^o}{k_B T}} \right]^{N_{ag}} \tag{12}$$

Now, χ_1 simply cannot be greater than $e^{-\frac{\mu_1^o - \mu_{N_{ag}}^o}{k_B T}}$, as $\chi_{N_{ag}}$ cannot be greater than 1. Hence, the CAC is given by

$$\begin{aligned} \chi_1^{\text{CAC}} = \sigma_{\text{PVA}}^{\text{CAC}} = \text{CAC} &\approx e^{-\frac{\mu_1^o - \mu_{N_{ag}}^o}{k_B T}} \\ &\approx e^{-\frac{\alpha(N_{ag}-1)}{N_{ag}}} \\ &\approx e^{-\alpha} \text{ for large } N_{ag} \end{aligned} \tag{13}$$

If we assume that the concentration of both PVA and PEG in the unfrozen water channels between the growing ice crystals (see main text) would be much (100 times) higher compared to the initial concentration, we obtain the result depicted in Fig.*S4*: the volume fraction of the PVA in these conditions brings the solution in a regime which is very close to the CAC - for concentrations of PEG of the order of 500 g/L. This qualitative finding is consistent with the experimental evidence (see main text) indicating that there exists a certain concentration of PEG beyond which the ice re-crystallisation inhibition activity of PVA does not increase anymore: this can be understood in terms of the CAC, as above the latter the overwhelming majority of the PVA particles in solution would have formed aggregates already.

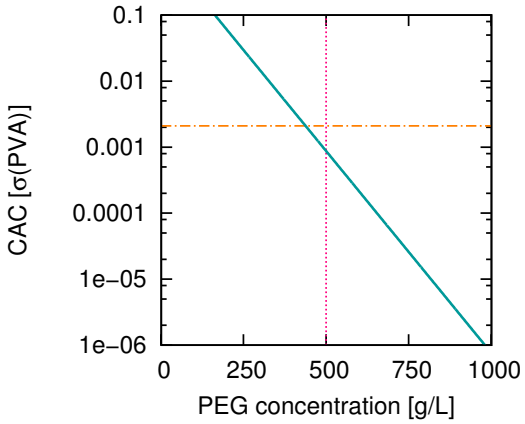

Figure S4. *Critical aggregation concentration (CAC) for PVA particles in terms of their volume fraction $\sigma(PVA)$ - as a function of the concentration of PEG in the solution. Assuming the concentration of both PVA and PEG in the unfrozen water channels between the growing ice crystals (see main text) is about two orders of magnitude higher compared to the original dilutions, a PEG concentration of 500 g/L (pink vertical line) would bring the PVA very close to its CAC (the volume fraction of PVA corresponding to these "icy" - i.e. high concentration - condition is indicated by the orange horizontal line).*

Qualitative insight

The number of assumption we needed to obtain some insight into the thermodynamics of PVA aggregation due to the depletion forces originating by small PEG particles prevents us to claim any quantitative understanding of this phenomenon. As a start, the discussion above is based on the Asakura-Oosawa model,[9–12] which, despite its popularity in biophysics, relies on the assumption of non-deformable, non-interacting particles. While the effect of charges can be included[9] and particles of different morphology can be taken into account,[13] at this stage we are not in a position to be able to measure with sufficient accuracy the volume fraction of PVA and PEG in solution, nor their exact morphology (particularly in terms of asphericity) and degree of aggregation. Nonetheless, our analysis provide robust qualitative insight suggesting that indeed depletion forces may be a strong driving force for the aggregation of large enough ice-binding agents / cryoprotectants in the presence of small enough depletants. As discussed in the main text, this evidence paves the way toward an especially intriguing strategy to boost the ice re-crystallisation inhibition activity of the next

generation of cryoprotectants.

References

(1) Phillips, D. J.; Congdon, T. R.; Gibson, M. I. Activation of ice recrystallization inhibition activity of poly(vinyl alcohol) using a supramolecular trigger. *Polym. Chem.* **2016**, *7*, 1701–1704.

(2) Stubbs, C.; Congdon, T. R.; Gibson, M. I. Photo-polymerisation and study of the ice recrystallisation inhibition of hydrophobically modified poly(vinyl pyrrolidone) co-polymers. *Eur. Polym. J.* **2019**, *110*, 330–336.

(3) Weisstein, E. W. Sphere-Sphere Intersection. http://mathworld.wolfram.com/Sphere-SphereIntersection.html.

(4) Marenduzzo, D.; Finan, K.; Cook, P. R. The depletion attraction: an underappreciated force driving cellular organization. *J. Cell Biol.* **2006**, *175*, 681–686.

(5) Marenduzzo, D.; Micheletti, C.; Cook, P. R. Entropy-Driven Genome Organization. *Biophys. J.* **2006**, *90*, 3712–3721.

(6) Novo, M.; Freire, S.; Al-Soufi, W. Critical aggregation concentration for the formation of early Amyloid-β (1–42) oligomers. *Sci. Rep.* **2018**, *8*, 1783.

(7) Lu, Y.; Yue, Z.; Xie, J.; Wang, W.; Zhu, H.; Zhang, E.; Cao, Z. Micelles with ultralow critical micelle concentration as carriers for drug delivery. *Nat. Biomed. Eng.* **2018**, *2*, 318.

(8) Israelachvili, J. N. *Intermolecular and surface forces / Jacob N. Israelachvili*, 2nd ed.; Academic Press London; San Diego, 1991.

(9) Asakura, S.; Oosawa, F. On Interaction between Two Bodies Immersed in a Solution of Macromolecules. *J. Chem. Phys.* **1954**, *22*, 1255–1256.

(10) Asakura, S.; Oosawa, F. Interaction between particles suspended in solutions of macromolecules. *J. Polym. Sci.* **1958**, *33*, 183–192.

(11) Moncho-Jordá, A.; Louis, A. A.; Bolhuis, P. G.; Roth, R. The Asakura–Oosawa model in the protein limit: the role of many-body interactions. *J. Phys. Condens. Matter* **2003**, *15*, S3429–S3442.

(12) Binder, K.; Virnau, P.; Statt, A. Perspective: The Asakura Oosawa model: A colloid prototype for bulk and interfacial phase behavior. *J. Chem. Phys.* **2014**, *141*, 140901.

(13) Galanis, J.; Nossal, R.; Harries, D. Depletion forces drive polymer-like self-assembly in vibrofluidized granular materials. *Soft Matter* **2010**, *6*, 1026.